IMAGING NANOSCALE POLLEN MORPHOLOGY WITH SUPERRESOLUTION STRUCTURED ILLUMINATION MICROSCOPY

BY

CASSANDRA J. WESSELN

THESIS

Submitted in partial fulfillment of the requirements
for the degree of Master of Science in Ecology, Evolution, and Conservation Biology
in the Graduate College of the
University of Illinois at Urbana-Champaign, 2015

Urbana, Illinois

Master's Committee:

Assistant Professor Surangi Punyasena, Chair
Assistant Professor Jessica Conroy
Professor Feng Sheng Hu
Research Assistant Professor Jon Marcot

ABSTRACT

Applications in the plant sciences that stem from disciplines as diverse as phylogenetics, physiology, and paleoecology all require ever-increasing imaging resolutions for accurate investigations of morphological hypotheses. Of these applications, the visualization of nanoscale plant morphology, such as the taxonomically diagnostic surface texture of individual pollen grains, is a special challenge for researchers. However, a combination of high-resolution imaging and computational analyses promises to unveil such nanoscale plant morphology for a whole spectrum of hypotheses, including those that address the taxonomic resolution of fossil pollen records. Therefore, the choice of imaging method for fossil pollen and hypothesized modern plant affinities is critical to research concerning the ecology and evolution of Earth's biomes. However, the options for visualizing such nanoscale plant morphologies that are smaller than the diffraction limit of light are often limited to electron microscopy, which presents significant disadvantages in routine palynological work compared to optical microscopy.

Superresolution Structured Illumination Microscopy (SR-SIM) is an emerging method that presents a powerful, non-destructive, and optically-sectioned way of imaging pollen that avoids certain disadvantages of electron microscopy. We examined and optimized the performance of SR-SIM in recovering the nanoscale surface morphology of the pollen of nine Poaceae species and compare our results to images obtained using Scanning Electron Microscopy (SEM) and an advanced transmitted light method: Laser-Scanning High-Resolution Differential Interference Contrast (LS-HR-DIC).

Through our comparisons of resulting images, we appreciated that SR-SIM, LS-HR-DIC, and SEM represent three very different imaging methods. SR-SIM uses fluorescence, LS-HR-DIC uses transmitted light, and SEM uses reflected electrons. Therefore, the results of our study

are expected in that the morphological information gathered by SR-SIM, LS-HR-DIC, and SEM is complementary, not identical: SR-SIM recovers three-dimensional features smaller than the diffraction limit, LS-HR-DIC produces diffraction-limited high contrast 3D representations, and SEM provides two-dimensional high-resolution images of an object's surface.

The morphological detail recovered from the SR-SIM is qualitatively comparable to the SEM. SR-SIM also represents an entirely new source of information on nanoscale plant morphologies, such as fine-scale pollen ornamentation and the interior structure of the pollen exine that could be used in conjunction with other standard approaches in optical and electron microscopy. SR-SIM is not a replacement for existing microscopic approaches, but is a viable alternative for material that is, by necessity or choice, mounted on microscopic slides.

ACKNOWLEDGMENTS

I am very grateful to so many people for supporting me throughout my graduate career. Endless thanks to my research adviser, Surangi Punyasena, for advising me through six years of research experiences as both an undergraduate and graduate student. Thanks to my committee members Jessica Conroy, Feng Sheng Hu, and Jon Marcot, for guidance and support. Additional thanks to Feng Sheng Hu for allowing me to use samples and equipment. Thank you so much to Mayandi Sivaguru (Shiv) and Glenn Fried at the Carl R. Woese Institute of Genomic Biology and Luke Mander at Open University for contributing significantly to the text and figures of this thesis. Further thanks to Shiv and Glenn for training me in the microscopy techniques explored in this thesis. A great many thanks to Michael Urban for training me in using equipment from the Hu Lab and for many insightful discussions. I express my sincere gratitude to the fellow students of the Punyasena Lab, especially Derek Haselhorst and Alejandra Restrepo, for both intellectual and emotional support throughout the completion of my research. Thank you so incredibly much to my fellow graduate students and dear friends, Christie Klinger and Kelsey Witt, for always being there for me during the completion of my degree. Finally, I extend all of my thanks and all my love to my family and friends for supporting me through everything and for always.

Funding for this research was provided by the National Science Foundation (Grants #1052997 and #1262561 to Surangi Punyasena). I am especially grateful to my Integrative Graduate Education and Research (Vertically Integrated Training with Genomics) Traineeship for not only providing the financial means for me to conduct research but also for the opportunity to study abroad at the Smithsonian Tropical Research Institute in Panamá.

TABLE OF CONTENTS

CHAPTER 1: IMAGING NANOSCALE POLLEN MORPHOLOGY WITH SUPERRESOLUTION STRUCTURED ILLUMINATION MICROSCOPY

Introduction

The ability to visualize the microscopic structure of plants is a fundamental need across the plant sciences. It is especially important for testing hypotheses that concern the taxonomic assignments of fossil pollen to modern botanical affinities. Most routine palynological investigations that examine changes in vegetation over time via the fossil pollen record involve the analysis of thousands of individual pollen grains. Such investigations are typically conducted using conventional brightfield transmitted light microscopy. This has been and continues to be a very popular technique because it allows morphological information to be acquired rapidly from many individual fossil specimens and is cost-effective (Traverse 2007; Sivaguru et al. 2012). However, the resolution of conventional optical microscopy techniques, which includes brightfield microscopy, is limited by the diffraction of light to 200–250 nm in most practical situations (Gustafsson 2000; Weiss 2000; Heintzmann and Ficz 2006; Huang et al. 2009; Schermelleh et al. 2010). This diffraction limit means that such techniques are unable to accurately capture morphological features of pollen that are less than 200–250 nm in size. In certain plant groups, notably the grasses, the morphological features that distinguish the pollen of different taxa are less than 200–250 nm in size, and in these cases the diffraction limit represents a fundamental barrier to recovering morphological information on which to base the improvement of the taxonomic resolution of fossil pollen records.

A recent review on the importance of taxonomic resolution of fossil pollen records concluded that a combination of high-resolution imaging and computational image analysis is the

best approach to improving taxonomic resolution (Mander and Punyasena 2014). Of the myriad of existing imaging techniques, electron microscopy has thus far represented the gold standard for high-resolution imaging and recovering nanoscale pollen morphology. Scanning Electron Microscopy (SEM) is capable of capturing features that are just a few nanometers in size and is widely used in palynology, but palynologists do not employ SEM to acquire images of large numbers of individual specimens in routine palynological investigations. This is due to several critical limitations of SEM. Specimens that are already mounted in microscope slides are often inaccessible without destruction of the slide, as are rare reference and fossil material that have been processed and preserved in oil. SEM imaging is also relatively time-intensive in comparison to optical microscopy (Fægri et al. 1989) and does not allow the user to switch between complementary imaging methods. In the case of palynology, this is especially important to do when additional morphological features are needed to refine taxonomic identification of pollen counts. Finally, SEM provides information only from the surface of a specimen and therefore cannot provide information on structures within the pollen wall (Traverse 2007). Another form of electron microscopy, Transmission Electron Microscopy (TEM), where electrons are transmitted through a thin-section of a specimen, can capture internal structures. In palynology, TEM is especially helpful in revealing the internal detail of the pollen exine that is not visible under traditional light microscopy techniques. However, preparation requirements limit its use in routine palynological work. In fact, to apply SEM, TEM, and light microscopy to just one specimen has been considered "something of a tour de force" given the associated preparation techniques and time requirements (Traverse 2007). All three techniques are rarely applied to large volume samples.

A classic example of pollen that needs both high-resolution imaging to distinguish its

nanoscale morphology and a routine method capable of working with its rich fossil record is grass pollen. When viewed using brightfield microscopy, grass pollen from across the whole family (Poaceae) appears spheroidal with a faint scabrate surface ornamentation and there are very few morphological characters that can be used to distinguish different taxa (Wodehouse 1935; Fægri et al. 1989; Beug 2004) (Figure 1). When viewed using SEM, however, pollen morphology across Poaceae is characterized by diverse and taxonomically significant patterns of surface ornamentation (Andersen and Bertelsen 1972; Page 1978; Peltre et al. 1987; Chaturvedi et al. 1998; Mander et al. 2013) (Figure 2). Despite this discovery, studies of grassland ecology and evolution are generally pursued using other Poaceae proxies such as silica-based phytoliths in lieu of pollen, mainly due to its morphological uniformity under transmitted light microscopy and the difficulty of applying SEM to large volume samples (Strömberg 2011). However, with high-resolution microscopy techniques that can increase the taxonomic resolution of fossil grass pollen and be applied to large volume samples, vast numbers of untapped fossil grass pollen records can be analyzed as completely new sources of paleoecological and evolutionary information. Taxonomically resolved fossil grass pollen records provide independent tests of paleoecological and evolutionary grassland hypotheses based on the phytolith record and add to the multiproxy approach that is key in corroborating such hypotheses.

In an attempt to addresses the issues inherent to electron microscopy while also improving the taxonomic resolution of pollen, we explore the ability of Superresolution Structured Illumination Microscopy (SR-SIM) to reveal nanoscale morphological information of pollen, with a special focus on grass pollen. We demonstrate that SR-SIM, an emerging optical superresolution microscopy method in the life sciences (Huang et al. 2010; Leung and Chou 2011; Han et al. 2013; Habuchi 2014; Long et al. 2014), is a viable technique for the recovery of

fine-scale pollen morphology. Within plant sciences, SR-SIM is known to augment studies of microscopic plant morphology, especially within plant cell biology (Fitzgibbon et al. 2010; Fitzgibbon et al. 2013; Liesche et al. 2013; Linnik et al. 2013; Komis et al. 2014; Sozzani et al. 2014; Rousseau et al. 2015), but to our knowledge this method has not been applied to the study of pollen morphology. Adopting such advances in imaging technology will allow palynologists to routinely examine morphological details that are hidden by the limited resolution of conventional optical microscopes, and fully exploit the wealth of palaeoecological and evolutionary information that is contained in pollen records.

Briefly, SR-SIM is a fluorescence technique with a light path similar to a widefield fluorescence microscope, but with an additional moving grid of parallel lines that is projected onto the sample in the lateral (XY) and axial (Z) directions. This allows the imaging of features smaller than the diffraction limit of light. Optical microscopy techniques like SR-SIM potentially provide a powerful combination of morphological data that is both nanoscale and optically-sectioned. These advanced microscopy techniques have the additional advantages of relative speed of imaging, the ability to work with existing slide-based material, and the convenience of allowing users to switch among complementary microscopy methods with the same material. We compare our results to another advanced optical microscopy technique, Laser-Scanning High-Resolution differential interference contrast microscopy (LS-HR-DIC). While diffraction limited, LS-HR-DIC produces images with higher resolution than typical DIC imaging due to the use of a coherent, single-wavelength laser light source. LS-HR-DIC images produce a 3D effect by shadowing one side of a feature, which is the result of the shear axis of light in the DIC technique. We investigated the ability of both SR-SIM and LS-HR-DIC to capture the fine scabrate ornamentation of grass pollen, which consists of granula and areolae

(polygonal areas separated by grooves that form a negative reticulum) (see (Punt et al. 2007) for terminology). We chose these features because aspects of their distribution and organization have been used in previous work to classify grass pollen grains below the family level with high accuracy (Mander et al. 2013). We used SEM images for our baseline comparisons (Figure 2).

Materials and Methods

Preparation of Pollen

We imaged nine species of grass pollen (Table 1), using the same specimens analyzed by (Mander et al. 2013). Pollen was isolated by breaking grass flowers collected from herbarium sheets and immersing them in H_2SO_4 followed by HCl, 10% KOH, 5% NaClO and HF. Specimens were mounted in silicone oil (refractive index 1.526) with a Zeiss high performance number 1.5 cover glass (18×18 mm, thickness 0.170±0.005 mm). SEM specimens were prepared by mounting individual pollen grains from ddH_2O onto a double-sided adhesive carbon disk that was attached to an SEM stub. The pollen grains were air-dried, and the stub was coated with ~10 nm of gold-palladium using a sputter coater. Specimens were viewed using a JEOL JSM-6060LV SEM (JEOL, Tokyo, Japan) at 15 kV (Mander et al. 2013).

Light Absorption Measurements of Pollen

We first measured the variation in the amount of light absorbed by each species of pollen to determine the extent to which absorption affects the recovery of morphological information. After setting the Köhler illumination, light absorption characteristics were analyzed for the pollen of nine grass species (Table 1) with three different wavelengths of light (405, 488 and 555

nm) using a laser-scanning microscope equipped with a transmission photomultiplier tube (Zeiss LSM 700 Confocal, Zeiss, Jena, Germany).

We measured mean intensity of the slide background at equally sized increments between 1-10% laser power to ensure a linear relationship between background mean intensity and laser power. The slide was then scanned for ideal pollen grains that were in equatorial position without any apparent damage. The selected pollen grains were positioned in the center of the field of view of a 20x Plan Apochromat 0.8 Numerical aperture (NA) objective with the focus on the center focal plane. Mean intensity measurements were based on six individuals per species. All settings, including laser power, were kept constant for each wavelength during mean intensity value acquisition.

Imaging Pollen with SR-SIM

SR-SIM utilizes a light path similar to a widefield fluorescence microscope (Figure 3), but with a moving grid of parallel lines that is projected onto the sample from the interference of the +1 and -1 diffraction orders produced by a grating in the light path. Moiré fringes created by the superimposition of the grid pattern and sample structure are larger than the diffraction limit and are transmitted through the microscope to the camera. Moving the resulting image from real space to Fourier frequency space then allows the original sample morphology to be reconstructed by removing the known grid pattern. This produces an image with features that are smaller than the diffraction limit of light (see (Gustafsson 2000; Gustafsson et al. 2008; Huang et al. 2009).

For example, 28 μm and 34 μm gratings are used to create near diffraction limited lines for 405 and 561 nm light, respectively, by combining the +1 and -1 diffraction orders in the back aperture of the objective. This pattern is rotated to either three or five angles and at each rotation

the pattern is moved five times to collect images with the grid in five phases, or positions. Thus, to construct a single plane of an SR-SIM image using five rotations and five phases per rotation, 25 images are acquired. For a typical pollen image of *c.*4.03 μm in thickness and with multiple sections taken at 130 nm steps, *c.*775 images are required for acquisition for a single wavelength of light. Because the grating projection is structured in the Z direction for optical sectioning, the axial resolution increases by a factor of two compared to confocal. Therefore, resolutions of 120 nm laterally (XY axes) and 250 nm axially (Z axis) can be achieved with SR-SIM, compared to a normal optical resolution of 250 nm laterally and 500 nm axially. This increased high frequency information is responsible for the improved resolution in SR-SIM over widefield fluorescence (Figure 4a-b). Additional explanation of how the SR-SIM achieves higher lateral and axial resolution can be found in (Gustafsson 2000; Gustafsson et al. 2008; Kasuboski et al. 2012; Jost and Heintzmann 2013; Allen et al. 2014; Dan et al. 2014; Long et al. 2014).

The Zeiss Elyra S1 SR-SIM system was calibrated for a 63x Plan Apochromat (1.4NA) oil objective using point spread function (PSF) measurements from both sub-diffraction (50 nm) and near diffraction (170 nm) limited point source fluorescent beads supplied from the system manufacturer (Figure 5). The PSF refers to the image of each sub-diffraction and near diffraction fluorescent point source that defines the spatial resolution of the microscope (Jost and Heintzmann 2013; Allen et al. 2014; Habuchi 2014). It can be estimated theoretically, based on the optical properties of the objective, or it can be measured experimentally through the imaging of uniform beads of known parameters. The EMCCD (Andor iXon 885) gain and exposure time were kept constant across species, but the laser power was set to optimize the quality of the image.

Most superresolution techniques are based on fluorescence, and use either the nonlinear

interaction of light with a sample, or the precise localization of individual particles or molecules within a sample (Heintzmann and Ficz 2006). Common superresolution microscopy techniques such as STORM and PALM are single-molecule localization-based superresolution techniques that use photoactivatable probes to activate individual components of the sample at different times during image acquisition (Han et al. 2013). With something that naturally exhibits autofluorescence at all times, like the pollen exine, these techniques do not work. In fact, the use of superresolution in the study of autofluorescent plant structures, like the strongly autofluorescent exine of pollen, has been limited, in part because these structures cannot be labeled with fluorophores or nano quantum dots (Dubertret et al. 2002). However, alternative superresolution methods, such as SR-SIM, work well with objects that autofluoresce across a range of frequencies, and so can be applied to imaging pollen and spores (Sivaguru et al. 2012).

Variation of SR-SIM Acquisition and Processing Parameters

We experimented with default acquisition and processing parameters of the SR-SIM software Zen to test the effects that the variation causes on resulting image quality (Zen Black module, Zeiss, Jena, Germany). The analysis of three main parameters from this analysis are included here: the number of illumination grating rotations in image acquisition; the use of an experimental versus theoretical PSF in the SR-SIM processing of images; and the use of post-image processing to improve contrast (baseline cut or shifted). From the resulting images, we made visual, qualitative assessments of image quality.

Image Visualization with SR-SIM

Following SR-SIM image acquisition, the resulting collection of optical sections was processed under default parameters or alternate parameters in the SR-SIM software Zen, depending on the experiment. Because creating a 3D projection using all the collected focal planes often resulted in poor image quality, we instead used a subset of the available focal planes that eliminated excess out of focus light resulting from the entire stack of planes. This subset best illustrated the pollen surface texture. We created a maximum intensity projection image of this subset to use as our final image. A 3x3 median filtering was then applied to the maximum intensity projection to remove noise speckles and this resulting image was saved under the visually optimal min/max display setting. The external and internal morphological detail revealed by SR-SIM was determined qualitatively by visually comparing the collected images.

Imaging Pollen with LS-HR-DIC

Unlike SR-SIM, LS-HR-DIC is a diffraction-limited technique. However, LS-HR-DIC produces images with higher resolution and greater contrast than typical DIC imaging due to the use of a coherent, single-wavelength laser light source. Moreover, LS-HR-DIC has higher resolution than typical brightfield due to the superior optical transfer function of DIC for nanometer scale features (Inoué and Spring 1997). The LS-HR-DIC light path that we have used in this study is shown in Figure 3.

A 100x Alpha Plan Apochromat DIC (1.46NA) objective was used in conjunction with a 1.4NA DIC slider and a 1.4NA Achromatic Condenser in a Zeiss LSM 710 microscope with a Hamamatsu Multialkali Photomultiplier Tube detector for visualizing the specimen. After setting the Köhler illumination, the DIC components (the polarizer and a Wollaston/Nomarski prism)

were placed above the specimen. The 1.4NA DIC slider (placed below the objective) was used to set the shear axis of the light and was kept at an approximately similar location across all species. Single focal plane images at the best contrast focal plane as well as series of 2D images covering the entire surface were captured using the automatic Z modality with optical sections taken at fixed 100 nm steps perpendicular to the axial plane. We have optimized the settings for this established technique by using a coherent, single-wavelength laser light source, a 1.4NA condenser, and silicone oil as our mounting medium.

Image Visualization with LS-HR-DIC

The final LS-HR-DIC images were background equalized in the program Autoquant X3 (Media Cybernatics, Bethesda, MD). A Fast Fourier Transformation (FFT) was applied to remove reflection fringes of the 405 nm laser using ImageJ (Schneider et al. 2012). Then minimum and maximum intensities were adjusted and set in Autoquant X3 to display the full dynamic range of intensities.

Results

Light Absorption Characteristics of Pollen and Effect of Wavelength on SR-SIM Images

Of the tested wavelengths of light (405, 488, and 555 nm), grass pollen absorbed the shortest wavelength (405 nm) the most and the longest wavelength (555 nm) the least with the middle wavelength absorption (488 nm) falling in between the extremes (Figure 6 top). Higher degrees of 405 nm absorption are also illustrated in the need to use higher laser power to recover morphological detail (Figure 6 bottom).

We compare results from the absorption extremes (405 and 555 nm) to test the effects of light absorption on SR-SIM performance. The excitation photon loss, or absorption of light by pollen, was between 50 and 70% for most of the pollen species at 405 nm and between 40 and 50% for most of the pollen species at 555 nm, with few exceptions (Figure 6 top). The most extreme outliers from this general trend are *Stipa tenuifolia*, which sustained *c.*20% excitation photon loss at 555 nm, and *Themeda avenacea,* which absorbed over 60% of light at 405 nm. We expected that lower degrees of absorption and excitation photon loss would lead to better contrast among morphological details recovered in the SR-SIM. For the pollen of all the species here, this was the case. All of the species of pollen absorbed light to a lesser degree using 555 nm compared to 405 nm (Figure 6 top), and SR-SIM images better resolved granula and areolae using 561 nm than 405 nm (Figure 7). In particular, it is apparent that both the resolution and signal to noise ratio (SNR), which is likened to contrast and defines how clear the image is, are better in images acquired using 561 nm excitation light than in images acquired using 405 nm excitation light (Figure 7). Between the two wavelengths, the 561 nm SR-SIM images of all species best reveal both the areolae and granula on the surface of the pollen (Figure 7). In contrast, the 405 nm wavelength performed poorly across most of the grass species investigated (Figure 7).

Overall Performance of SR-SIM

Visual comparison of SR-SIM and SEM images of grass pollen surface texture indicate that the SR-SIM instrument does not produce images of the granula and areolae that correspond exactly to SEM images of these morphological features. For example, individual granula on the surface of *S. tenuifolia* appear to have subtle texture when imaged using the SR-SIM, but these

structures appear smooth when viewed using the SEM (Figure 2; Figure 8). For some species, like *T. avenacea*, *Oplismenus hirtellus*, and *Dactylis glomerata*, which have well-defined features according to SEM (Figure 2), the granula that ornament the areolae are well resolved, and the boundaries of the areolae are sharp in SR-SIM images (Figure 8). In other cases, however, such as with *Sporobolus pyramidalis* and *Poa australis*, the boundaries of the areolae are sharp in the SEM images but are less clear in the SR-SIM images (Figure 2; Figure 8).

Effect of SR-SIM Image Acquisition and Processing Parameters

As discussed previously, SR-SIM images are acquired through the movement of structured illumination grating patterns, and there is the option of either five or three structured illumination grating rotations. The five rotations option requires 25 images to create a single SR-SIM optical section while the three rotations option only needs 15 images. While five rotations provide more morphological information due to more rotations resulting in an isotropic improvement in resolution at all angles, the degree of photobleaching may also increase, thus leading to low SNR and poor image quality. Our results indicate that restricting ourselves to three rotations negatively affected the recovery of areolae and granula by reducing the SNR for most of the species investigated (Figure 9). There are few instances where the SNR remained the same between rotation options (i.e. *S. tenuifolia, Phalaris arundinacea,* and *O. hirtellus*), and one instance where three rotations actually improved the resolution of areolae (i.e. *S. pyramidalis*).

The PSF, which is a part of the SR-SIM image processing, is also used in the deconvolution of out-of-focus light within an image (Malkusch et al. 2001). An experimental PSF measured through the imaging of uniform beads of known parameters should more

accurately discriminate between signal and noise than a theoretical PSF based on the optical properties of the objective because it would more accurately account for the actual optical properties of the system. However, if the signal of the pollen surface ornamentation falls in the same frequency as the noise that is deconvoluted and deblurred, then both signal and noise may be removed with experimental PSF processing. This might result in poor recovery of surface texture. Results for using experimental PSF processing varied among species and between areolae and granula. For *S. tenuifolia* granula recovery, the use of an experimental PSF has positive influences due to an improvement in SNR (Figure 9). For other species such as *T. avenacea* and *D. glomerata*, however, granula recovery suffers under experimental PSF processing. In the case of *P. arundinacea*, areolae are better recovered with the experimental PSF processing, but granula recovery suffers (Figure 9).

Post-imaging processing involving the image baseline can be used to improve image quality. The baseline cut mode automatically removes light frequencies included in the image background and produces an image with a dark background. On the other hand, in the baseline shifted processing mode, the user can instead manually remove the background. We find that with baseline-shifted processing, in which we have the control to adjust the background of the image, there is a positive impact on the recovery of areolae in *Digitaria insularis* and both the granula and areolae of *D. glomerata, D. insularis*, *O. hirtellus* and *T. avenacea* (Figure 9), where baseline cut removed too much signal from the image.

Overall Performance of LS-HR-DIC

Fast Fourier analyses (which transform an image into its frequency representation) of brightfield, widefield DIC (incoherent light source), and LS-HR-DIC (coherent light source)

show that the LS-HR-DIC technique transfers more high frequency information to the final image and, consequently, has higher resolution than brightfield and widefield DIC in the direction of the prism axis (Figure 4c-d). Additionally, the LS-HR-DIC and SEM images of grass pollen surface texture show close correspondence. The negative reticulum that characterizes species such as *D. glomerata* and *O. hirtellus* is as well defined in the LS-HR-DIC images as the SEM images, and the margins of the areolae themselves are quite sharp (Figure 8). In all species that have an areolate surface texture (*D. glomerata*, *D. insularis*, *O. hirtellus*, *S. pyramidalis*, *P. australis*, and *T. avenacea*), the LS-HR-DIC technique recovers structures that appear nearly identical to the granula that ornament areolae in the SEM images of these species (Figure 2; Figure 8). However, due to the diffraction limit, it is unclear whether all of the granula are fully resolved, or whether some of these structures represent two or more overlapping granula, in a situation similar to two overlapping airy disks. Some of the larger granules on the surface of *P. australis* and *O. hirtellus* in the LS-HR-DIC image could be examples of such overlap (Figure 8). The linear features that are visible in the LS-HR-DIC image of *A. odoratum* also likely represent several unresolved granules (Figure 8).

Discussion

Images of grass pollen surface texture acquired using the SR-SIM, which are twice the resolution of conventional optical microscopy (120 nm), indicate that this instrument can capture taxonomically significant morphological features that are too small to be resolved using conventional brightfield transmitted light microscopy. These results showcase how advanced microscopy techniques add to the existing arsenal of imaging methods for researchers interested in the analysis of nanoscale plant morphologies, such as pollen ornamentation. In the case of

grass pollen, these features include scabrate ornamentation consisting of granula and areolate ornamentation composed of polygonal areas separated by grooves that form a negative reticulum (Mander et al. 2013). SR-SIM images provide three-dimensional information on these morphological features as well as those features located internally to the pollen wall. A Euphorbiaceae species known to have complex reticulate patterning of the clava illustrates how the clava arrangement can be better visualized with optical sectioning (Figure 10).

Our results demonstrate that in certain cases, SR-SIM and LS-HR-DIC can qualitatively recover fine-scale morphology that is comparable and complementary to that captured by SEM (Figure 2; Figure 8). However, these images do not contain enough contrast, that is they have too poor of a SNR, to extract quantitative morphological data that is key to classifying grass taxa (Li and Mio, unpublished analysis, following Mander et al. 2013). Recent experimental work initiated by collaborators Mayandi Sivaguru and Glenn Fried at the Carl R. Woese Institute of Genomic Biology shows that a combination of additional fluorescent labeling of pollen specimens, minimal acid processing, an aqueous-based mounting media, and shallow slide mounts results in SR-SIM grass images with greatly improved contrast (Figure 11). Such images capture nanoscale pollen morphology much better than unlabeled, processed pollen mounted in oil (Figure 8; Figure 11). The details of the areolae and granulae in Figure 11 are closer to what the SEM provides compared to other techniques (Figure 2; Figure 8; Figure 11). This ongoing work explores more effective specimen preparation methods for SR-SIM imaging and encourages further investigation into the possibilities of SR-SIM recovering quantifiable grass morphology for taxonomic classification. Moreover, it is important to note that the original SR-SIM procedures described herein may still be valuable for researchers who wish to image pollen collections with the SR-SIM that are already mounted in oil.

SR-SIM, LS-HR-DIC and SEM all captured key diagnostic features of the grass pollen exine to different degrees of success, with the SEM capturing quantifiable morphology (Mander et al. 2013). The morphological information represented by these different techniques is complementary, not identical. Further experimentation with the specimen preparation protocol used in Figure 11 is needed to produce SR-SIM images with a high enough SNR for comparing morphological quantification capabilities with SEM. Therefore, according to the results of this study, the appropriateness of a given technique for the study of pollen morphology ultimately will not only depend on the morphological characters of interest, the light absorption characteristics of the pollen grain itself, and image acquisition and processing parameters, but also on the effectiveness of pollen preparation methods.

Optimizing the SR-SIM

Several acquisition and image processing factors affected our ability to resolve the surface texture features of grass pollen with the SR-SIM. One of the acquisition factors is that there is a physical limitation to the SR-SIM itself that originates from the grating sizes used with each excitation wavelength, which are projected as grids in the Z-dimension. If the surface texture feature of a pollen grain (i.e. areolae and/or granula) is smaller than the Z-resolution of a given grating size, then the SR-SIM cannot physically resolve that particular morphological feature as the pollen is moved to and from the illumination pattern during optical sectioning (Figure 12). For example, the texture of *A. odoratum* is poorly resolved by the SR-SIM (Figure 8) most likely due to the shallowness of its areolae and granula compared to the grating size (as seen in the lack of intensity difference among features in SEM, Figure 2). Conversely, the taller

areolae and granula of *T. avenacea*, *D. glomerata*, and *O. hirtellus* (as seen in SEM, Figure 2) allow it to be imaged clearly with the SR-SIM (Figure 12).

Our results also indicate the extent to which the wavelength of excitation light used during image acquisition exerts a major control on the representation of grass pollen surface texture. We suggest that the lower SNR in images acquired using a shorter wavelength of incident light is due to comparatively greater absorption of shorter wavelengths of light by the grass pollen exine (Figure 6; Figure 7). There is a higher SNR in images acquired using a longer wavelength due to the comparatively lesser absorption of longer wavelengths by grass pollen (Figure 6; Figure 7). Previous work has shown that the pollen exine absorbs more short than long wavelengths of light (Sivaguru et al. 2012), and we found a similar pattern with the species of grass pollen investigated here. While pollen absorbs shorter, higher energy wavelengths of light (most likely for protection against DNA damage (Lomax et al. 2008; Atkin et al. 2011)), such absorptive and protective properties of pollen are unfortunately detrimental in resolving fine surface texture due to the destructive effect that absorption and light scattering have on the SNR of the resulting image. Although shorter wavelengths of light in SR-SIM microscopy theoretically produce better image resolution (Sivaguru et al. 2012), this advantage is negated when imaging grass pollen due to the high absorption of shorter wavelengths of light.

In further regards to deviating from acquisition parameters, the researcher should seek to maximize the number of grid rotations performed to maximize the morphological detail recovered. This should only be reduced if the morphology is robust enough to be visible with only three rotations, or where photobleaching is a significant concern. We hypothesize that the number of rotations does not negatively affect species like *S. tenuifolia* and *O. hirtellus* (Figure

9) because their well-defined, inherently high contrast granula and areolae (Figure 2) may be sufficiently recovered with three rotations.

Alternative processing parameters such as experimental PSF and baseline-shifted processing are needed due to differences in morphology among species. For example, a pollen grain with a more complicated topography characterized by taller, relatively uneven granula and areolae (e.g. *T. avenacea* and *D. glomerata*) potentially have a broader spectrum of signal frequencies than a pollen grain with very simple topographic features (e.g. *A. odoratum*). As a result, the resolvability of both areolae and granula may be differentially affected by these processing parameters (Figure 9). This is because both experimental PSF and baseline-shifted processing depend upon removing and/or keeping certain frequencies belonging either to signal or to noise. As we demonstrated, the morphological features of pollen grains with complicated topographies are often poorly resolved under experimental PSF processing due to the excessive removal of signal frequencies shared with the removed noise of out-of-focus light (Figure 9). Those same morphological features are improved by application of baseline-shifted processing because we have better control in adjusting the amount of morphological signal conserved when removing background noise (Figure 9). Therefore, there is not a single optimal setting for pollen imaging. The choice of using experimental PSF or theoretical PSF processing for deconvolution and the choice of baseline-shifted or baseline-cut processing to remove background noise will vary based on the nature of the morphological features investigated. Performing both processing techniques takes approximately six minutes, so this is not an unreasonable approach to processing SR-SIM images.

Taken together, the default parameter settings of the Zeiss Elyra SR-SIM processing software provide a good start for retrieving pollen surface texture information, but due to many

differences in surface texture among species, and consequent differences in reactions to variations in default settings, it is advisable to try multiple processing techniques on a per case basis (Figure 9).

Correlations between SR-SIM and SEM

Establishing feature to feature correlations between superresolution images and scanning electron micrographs of biological structures is difficult because of the different sample preparation methods that are required for each technique (Kopek et al. 2012). Specimens imaged using SEM are coated in gold-palladium, which potentially obscures nanometric morphological details or introduces possible artifacts (e.g. (Muscariello et al. 2005)). Specimens prepared for SR-SIM analysis are not coated before imaging. Therefore, the texture that is evident on the individual granules in the SR-SIM images may represent real, nanoscale morphological detail, though this morphology may not be evident in an SEM image. Environmental scanning electron microscopy (ESEM), circumvents the potential artifacts introduced by coating a specimen due to its ability to image untreated samples. Despite this advantage, ESEM is not an appropriate microscopy technique for imaging grass pollen. Uncoated samples are more transparent to the electron beam, so produce less signal and therefore less contrast (Kirk et al. 2009). Less contrast and signal in the ESEM results in a poor image of the innately subtle morphological features of grass pollen. We observed this result in our own experiments (Wesseln, unpublished).

The nature of SEM and SR-SIM images are also very different. The SEM captures information from only the very surface of a specimen, whereas the SR-SIM, which relies on the fluorescence emission properties of sporopollenin, is potentially able to reveal intricate, internal structural differences. Due to the nature of optical sectioning in the SR-SIM, this internal

information is three-dimensional (Figure 10). As a result, some of the texture that is visible in the SR-SIM images of grass pollen that is not visible in the corresponding SEM images (such as that on the granules of *S. tenuifolia*, Figure 8) could represent morphological features that are located within specimens, rather than on their surface.

Finally, we must consider that SEM and SR-SIM may be better compared once an appropriate pollen preparation protocol has been established for improving the contrast among morphological features in SR-SIM images (Figure 11).

Correlations among SEM, SR-SIM and LS-HR-DIC

LS-HR-DIC captured high contrast, detailed images of both granula and areolae for most of the grass species investigated (Figure 8). One of the reasons why LS-HR-DIC may have worked so well with grass pollen is because it produces high contrast images of the relatively thin and transparent grass pollen exine. LS-HR-DIC uses transmitted light, so the opacity of an object will affect its performance (Sivaguru et al. 2012). In addition, because the pollen is mounted in silicone oil with a refractive index that matches glass, and immersion oil is placed both between the slide and microscope condenser and the slide and objective (Figure 3), the scattering loss of light due to the mismatch of refractive indices is minimized compared to other transmitted techniques. This allows a high frequency signal to pass through the objective. One can see that the LS-HR-DIC produces significantly more high frequency information than brightfield and conventional DIC techniques (4c-e).

LS-HR-DIC, however, does not capture as large a range or magnitude of frequencies as the SR-SIM (Figure 4b-c). The SR-SIM captures more high frequency, small sized features than any other technique as seen in Figure 4, therefore also indicating that the resolution of SR-SIM is

the best of all the techniques. Additionally, unlike SR-SIM, LS-HR-DIC images are not true three-dimensional, optically-sectioned data. However, there is an inherent variable depth of focus in the combination of 2D images at various focal planes, with which one could then create extended depth of focus (EDF) images (Figure 13). With EDF images, one can visualize surface texture with optical sectioning in the Z-direction. In addition to optically-sectioned EDF images, new, emerging techniques such as superresolution structured illumination DIC microscopy would potentially complement SR-SIM by combining the benefits of transmitted and reflected light microscopies (Chen et al. 2013).

Conclusions

In this study we illustrated the ability of SR-SIM and LS-HR-DIC to recover taxonomically diagnostic surface texture morphologies of grass pollen as well as the more robust morphologies of Euphorbiaceae pollen. The results demonstrate how optical microscopy can be used alongside electron microscopy to provide additional and complementary morphological information. A recent archaeological study reached the same conclusion in that optical and electron microscopy are best used as complementary methods for the most accurate interpretation of usewear and residues on stone tools (Borel et al. 2014).

We also suggest that the use of SR-SIM will be most useful and advantageous for pollen specimens already mounted in microscope slides, such as rare fossil pollen material or holotype reference specimens, or when users need to switch among complementary imaging techniques with the same material. Moreover, we recognize that further experimentation on how pollen is prepared for SR-SIM imaging is critical for improving this technique in its ability to capture quantifiable pollen morphology comparable to the SEM. Following improved protocol

development, if the SR-SIM can reveal quantifiable grass pollen morphology that results in the formation of morphological diversity clusters representative of real diversity, then the resolving power of the SEM is no longer necessary and the application of SR-SIM to large-scale paleoecological studies will be possible. By simply imaging fossil grass specimens on slides made from cores and then applying computational analyses to the resulting quantifiable morphology, morphological clusters representing a real measure of ancient grass diversity can be determined.

We reach three conclusions based on the work presented:

(1) Images of grass pollen surface texture acquired using the SR-SIM, which are twice the resolution of conventional optical microscopy (120 nm), indicate that this instrument can capture taxonomically significant morphological features that are too small to be resolved using conventional brightfield transmitted light microscopy. In the case of grass pollen, these features include scabrate ornamentation consisting of granula and areolate ornamentation consisting of polygonal areas separated by grooves that form a negative reticulum (Mander et al. 2013). SR-SIM images provide three-dimensional information on these morphological features as well as those features located internally to the pollen wall, as illustrated with the Euphorbiaceae pollen (Figure 10). For certain species, such as *S. tenuifolia*, which has inherently high contrast between its granula and exine background, the SR-SIM is able to capture the density and size of granula as recorded by the SEM and may even capture details of texture within the granula that are inaccessible to SEM. However, the surface texture of species with inherently low contrast areolae and granula, such as *A. odoratum*, cannot be resolved by the SR-SIM due to the wavelength and grating size limitations of the instrument. Moreover, as evidenced by the inability to quantify morphology from our SR-SIM images, there is overall poor contrast in SR-

SIM images taken of processed pollen prepared in oil with no additional fluorescent labeling. However, future experimental work promises to improve upon the SNR in SR-SIM images by adjusting how pollen specimens are prepared for imaging.

(2) SR-SIM acquisition and image processing parameters have major effects on the images of grass pollen surface texture obtained. In particular, the SNR is higher in SR-SIM images acquired using 561 nm excitation light than in those acquired using 405 nm excitation light (Figure 7). We suggest that this is a result of the absorption of shorter wavelengths of light by the grass pollen exine (Figure 6 top). The default processing routine in the SR-SIM algorithm is adequate for processing SR-SIM images, but changing certain parameters (i.e. from three to five rotations, from baseline-cut to baseline-shifted processing, or from theoretical to experimental PSF) may improve surface texture recovery depending on the species (Figure 9). Future work with optimizing SR-SIM imaging of pollen through changes in slide preparation is currently underway at the Carl R. Woese Institute of Genomic Biology at the University of Illinois.

(3) Images of grass pollen surface texture acquired using LS-HR-DIC show close correspondence with SEM images of the same. The correspondence between images of the negative reticulum and areolae that characterizes species such as *D. glomerata* and *S. pyramidalis* is particularly good (Figure 8). However, the granula that ornament the areolae of certain species are not always fully resolved and may appear as more linear features on the pollen surface as this technique is still diffraction limited (Figure 8). Additionally, this technique lacks three-dimensional information on pollen surface ornamentation patterns. However, use of an EDF image compiled of multiple planes may provide additional morphological information in the Z direction (Figure 13).

FIGURES AND TABLES

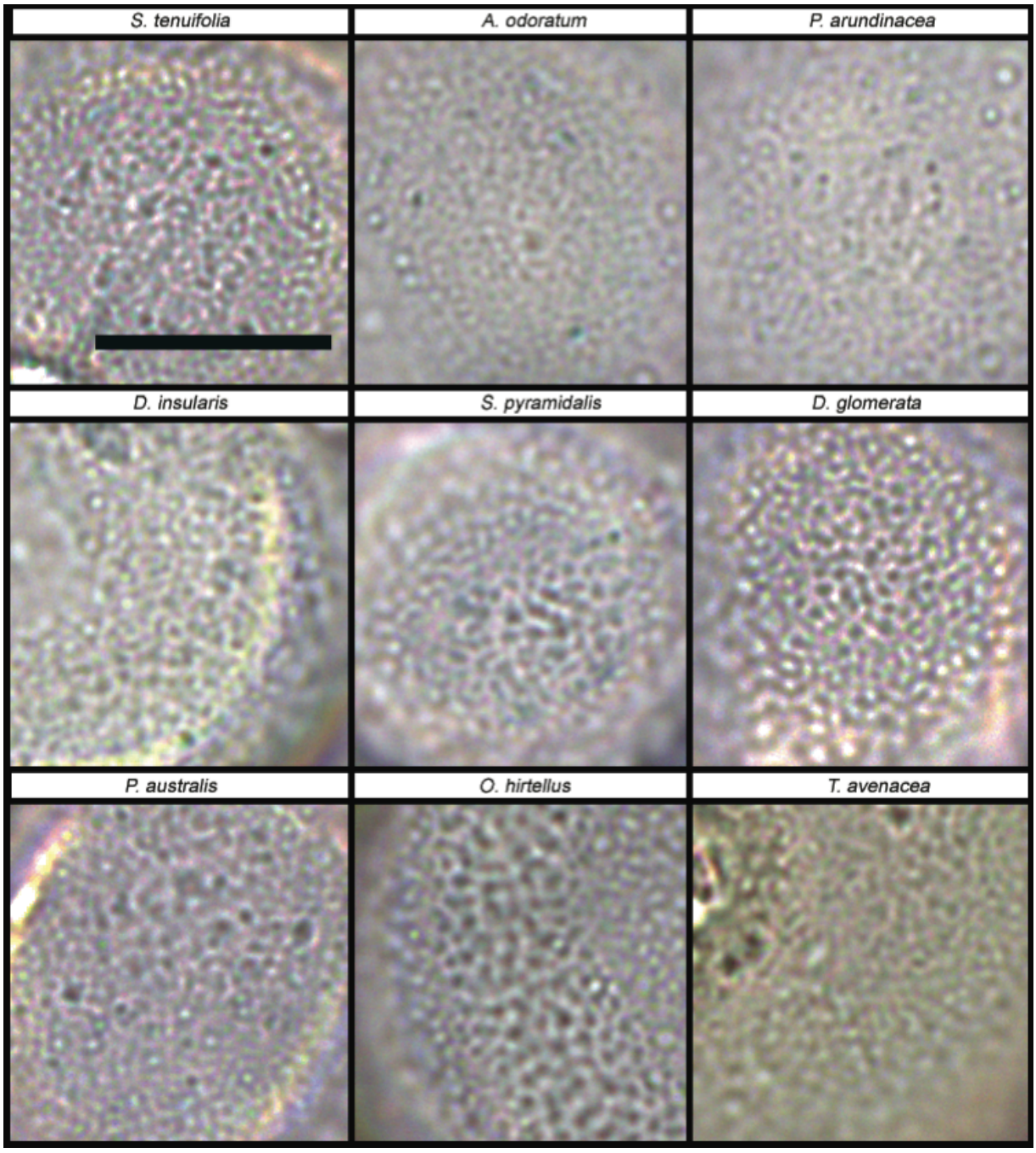

Figure 1. Brightfield images of the pollen of nine grass species taken with a Zeiss transmitted light microscope at 100x, illustrating the morphological uniformity of grass pollen under transmitted light optical microscopy. Scale bar represents 10 μm.

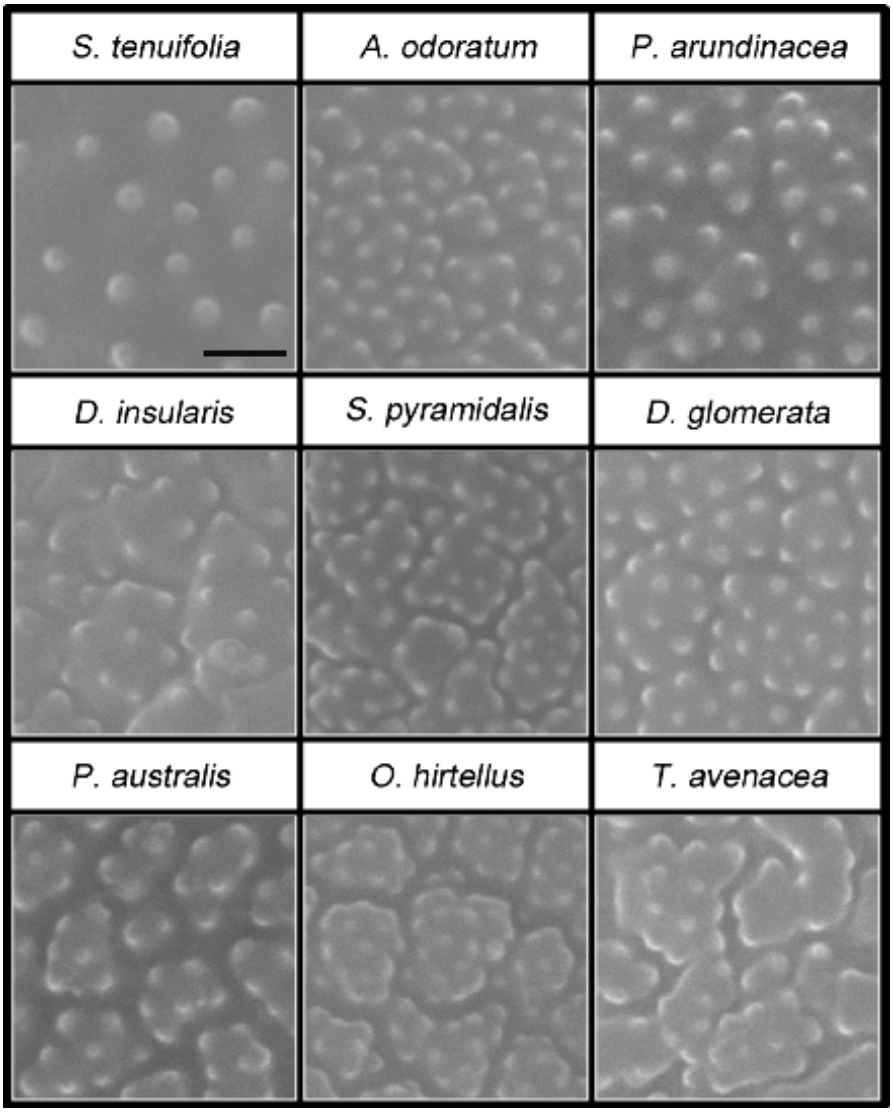

Figure 2. Scanning electron microscopy (SEM) images of the pollen of nine grass species illustrating diversity of granula and areolae patterning. Images taken at x12000 magnification. Scale bar represents 1.4 micrometers. SEM images from University of Illinois IDEALS digital repository: https://www.ideals.illinois.edu/handle/2142/43358.

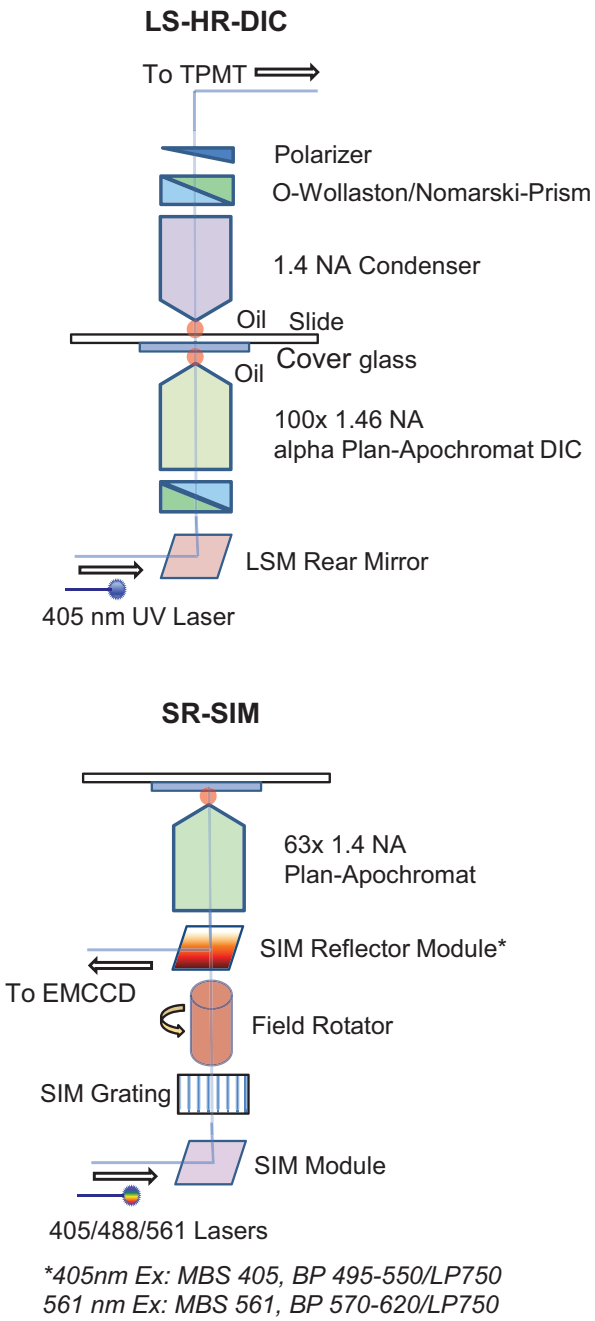

Figure 3. Experimental setup and light path used for Laser-Scanning High-Resolution Differential Interference Contrast (LS-HR-DIC) and Superresolution Structured Illumination Microscopy (SR-SIM) techniques compared in this study. Note that TPMT: Transmitted light Photomultiplier Tube, NA: Numerical aperture, EMCCD: Electron Multiplication Charge Coupled Device, MBS: Main Beam Splitter, BP: Band Pass, LP: Long Pass, nm: nanometer, and Ex: excitation.

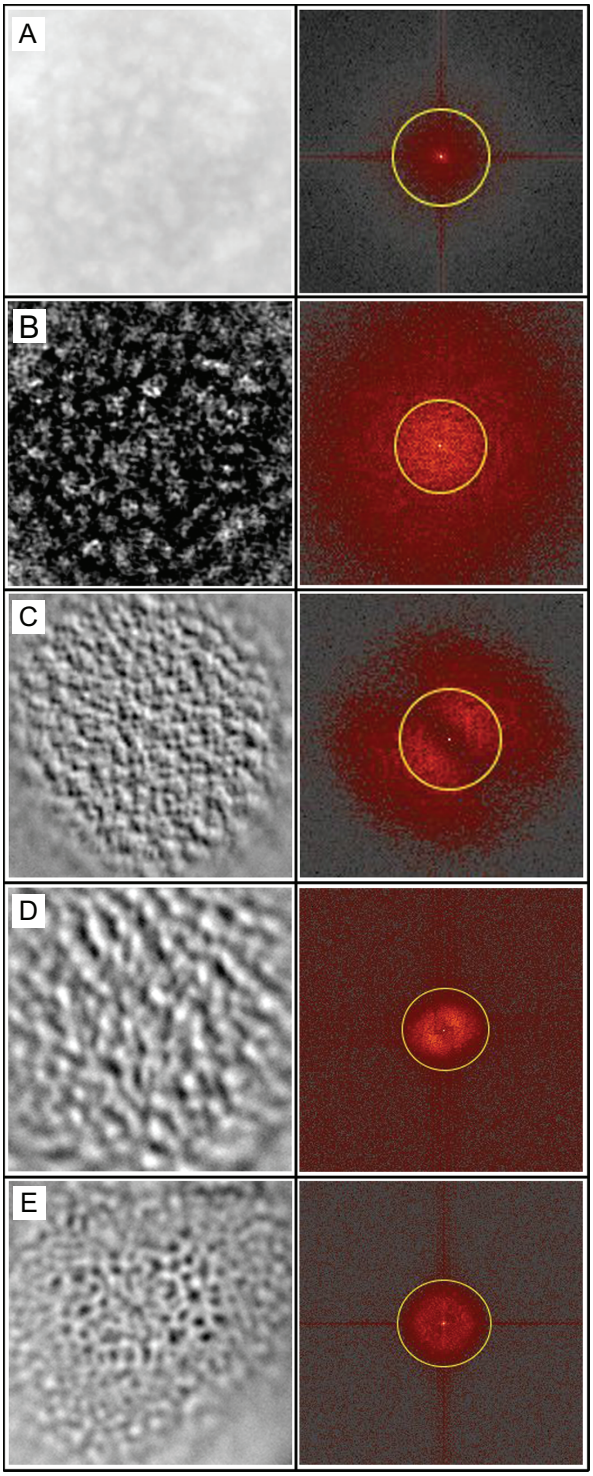

Figure 4. Comparison of resolution capabilities of microscopy techniques using corresponding Fast Fourier transformed (FFT) images of *Dactylis glomerata*: (a) widefield fluorescence; (b) Superresolution Structured Illumination Microscopy (SR-SIM); (c) Laser-Scanning High-Resolution differential interference contrast (LS-HR-DIC); (d) widefield high contrast differential interference contrast (WF-HC-DIC); (e) brightfield. FFT translates an image from the spatial domain into its sin and cosine components in the frequency domain equivalent. In an FFT image, each point represents a particular frequency contained in the original image. The yellow circle indicates frequencies approximately at 400 nm/cycle, the typical resolution of an optical microscope, and the edge frequency of all FFT images are approximately 130 nm/cycle. Note that the SR-SIM (b) produces images with the most high frequency information. Widefield fluorescence (a) and brightfield (e) produce the least. Both LS-HR-DIC (c) and WF-HC-DIC (d) produce lobed frequency representations due to the differential transfer function of the DIC prism. Scale: (a, b) are 8 µm across; (c) is 7.8 µm across, and (d, e) are 13 µm across.

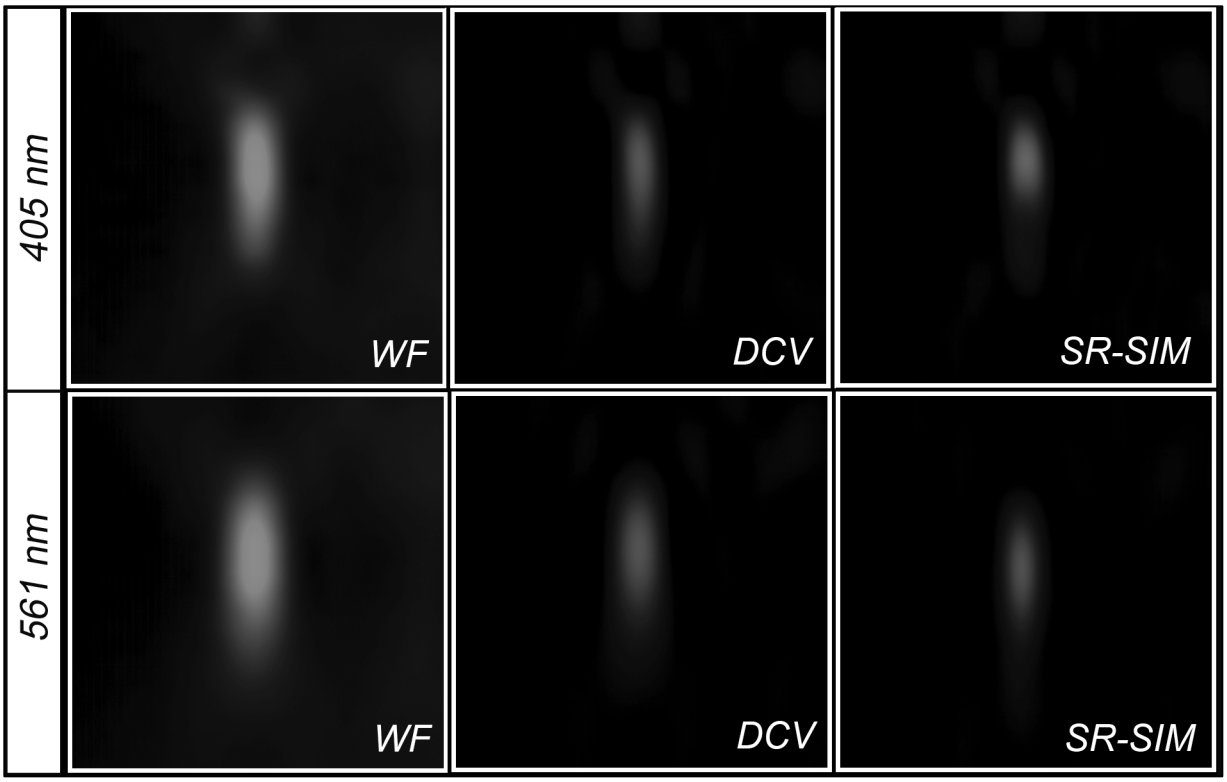

Figure 5. Comparison of measured point spread function (PSF) point sources (170nm) of widefield (WF), widefield plus deconvolution (DCV) and superresolution (SR-SIM) techniques. Figure includes XZ images of PSFs of a green and red fluorescent Tetraspeck bead (Zeiss Calibration Standard, 170 nm). PSF is a measurement of the scatter of light from a tiny point source of light (fluorescent bead): the less scattering of light and the smaller the PSF in both XY (not shown) and XZ (shown) directions, the better the resolution of the technique. The experimental resolution from full width at half maximum (FWHM) measurements is as follows: for 405nm, WF is 241 nm, DCV is 167 nm, SR-SIM is 137 nm; for 561 nm, WF is 280 nm, DCV is 198 nm, and SR-SIM is 157 nm.

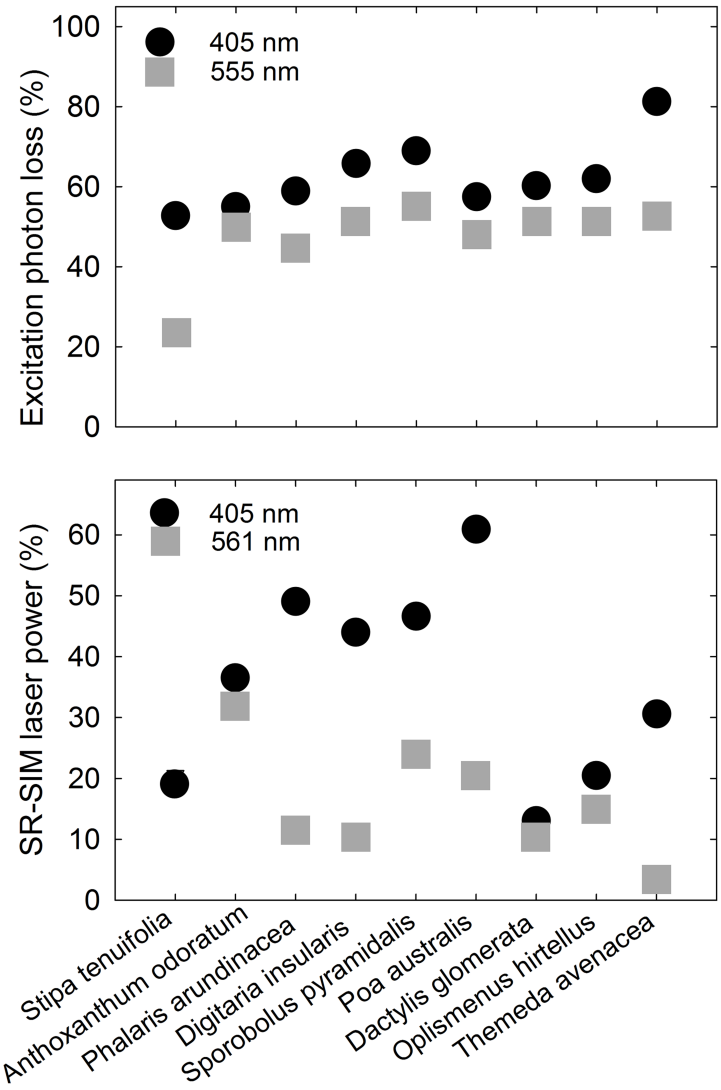

Figure 6. Excitation photon loss measured as a function of absorption of the pollen of all nine grass species at different wavelengths of light. Mean intensity values were subtracted from 100 to express the data in percent excitation photon loss. Though Superresolution Structured Illumination Microscopy (SR-SIM) utilizes a 561 nm laser, we considered the 555 nm laser of the Zeiss LSM 700 Confocal to be an adequate comparison. The second part of the figure depicts the laser power required to retrieve an optimal signal from pollen.

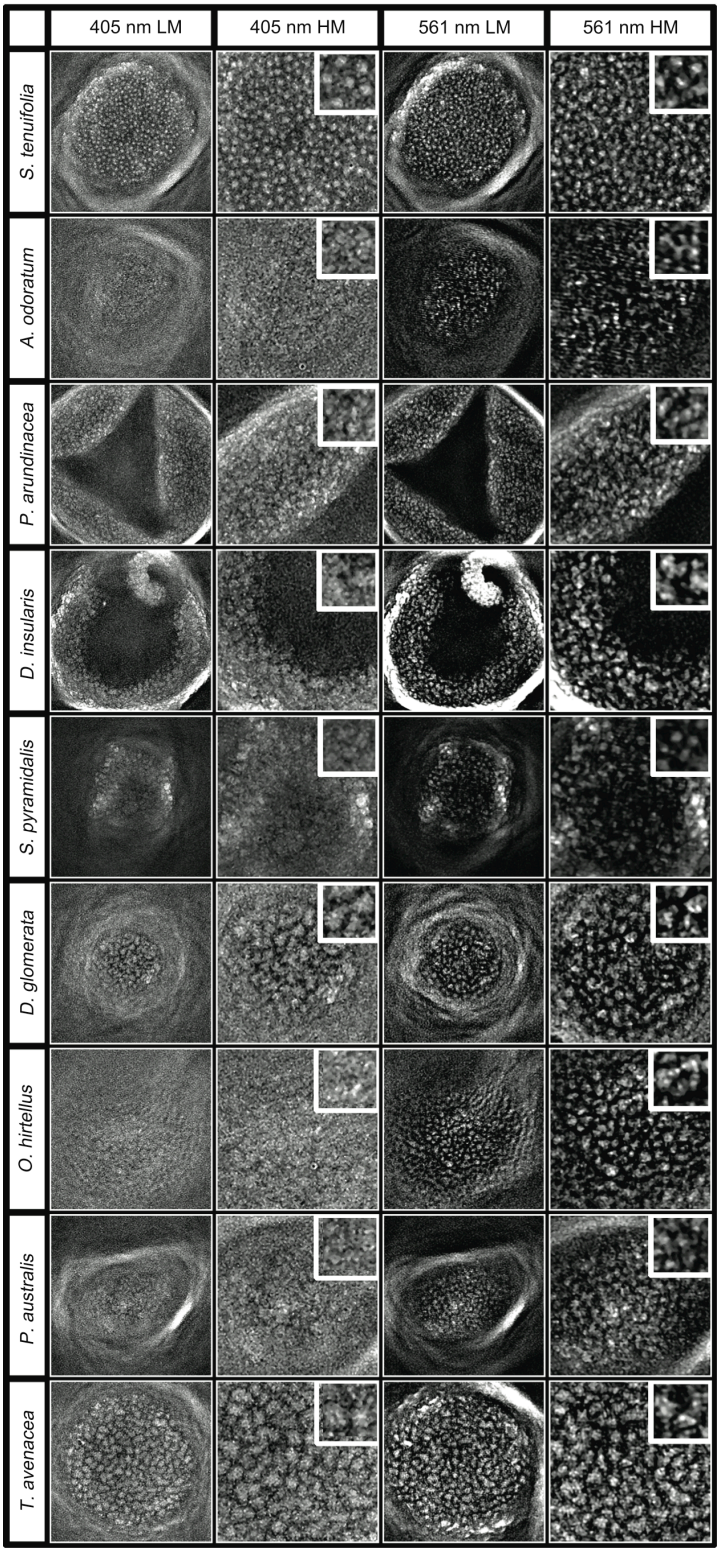

Figure 7. Superresolution Structured Illumination Microscopy **(**SR-SIM) images of nine different grass pollen species acquired using two different excitation wavelengths (405 and 561 nm). Scale: the low magnification (LM) images are 20 micron across, high magnification (HM) images are 10 µm across, and the insets are 2 µm across.

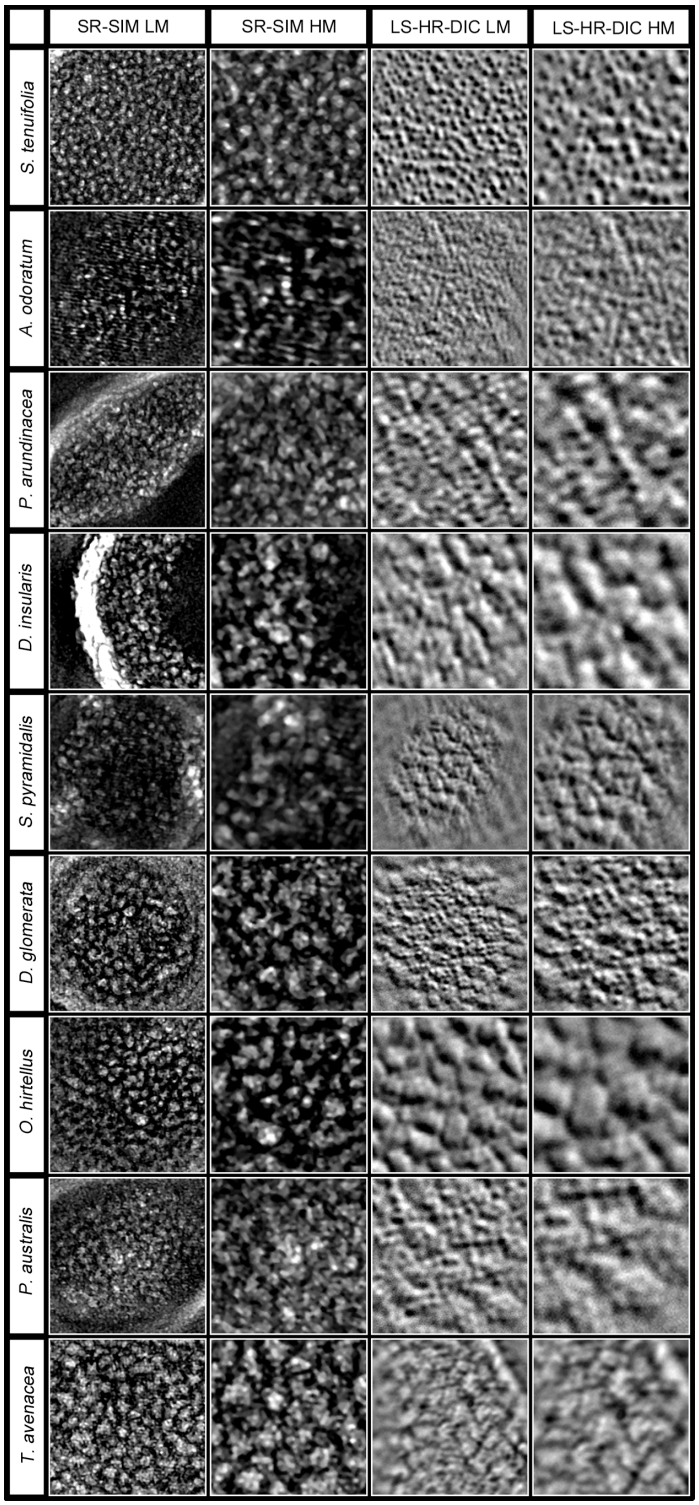

Figure 8. Comparison of grass pollen surface ornamentation as recorded by Superresolution Structured Illumination Microscopy (SR-SIM) and Laser-Scanning High-Resolution Differential Interference Contrast Microscopy (LS-HR-DIC). Images shown at low magnification (LM) and high magnification (HM). Scale: the LM images of SR-SIM are 10 µm across and the HM images are 3.6 µm across. The LM of LS-HR-DIC images are 10 µm across and the HM images are 5 µm across.

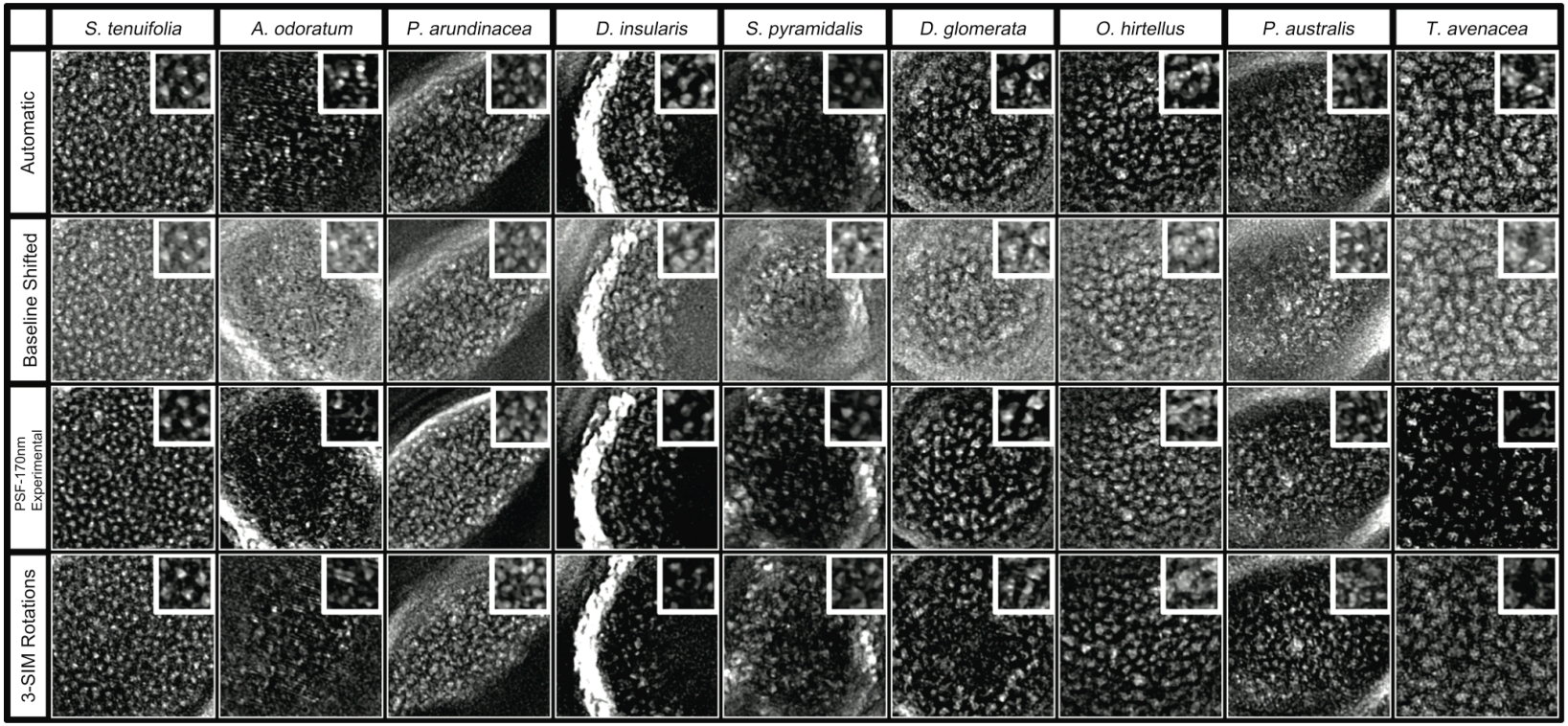

Figure 9. Superresolution Structured Illumination Microscopy (SR-SIM) performance of altered SR-SIM acquisition and processing parameters compared to the fully automatic (default) output (top row). All SR-SIM optimization processing was performed using the Zen Black (Zeiss, Jena, Germany) module. Scale: the images are 10 μm across and the insets are 2 μm across.

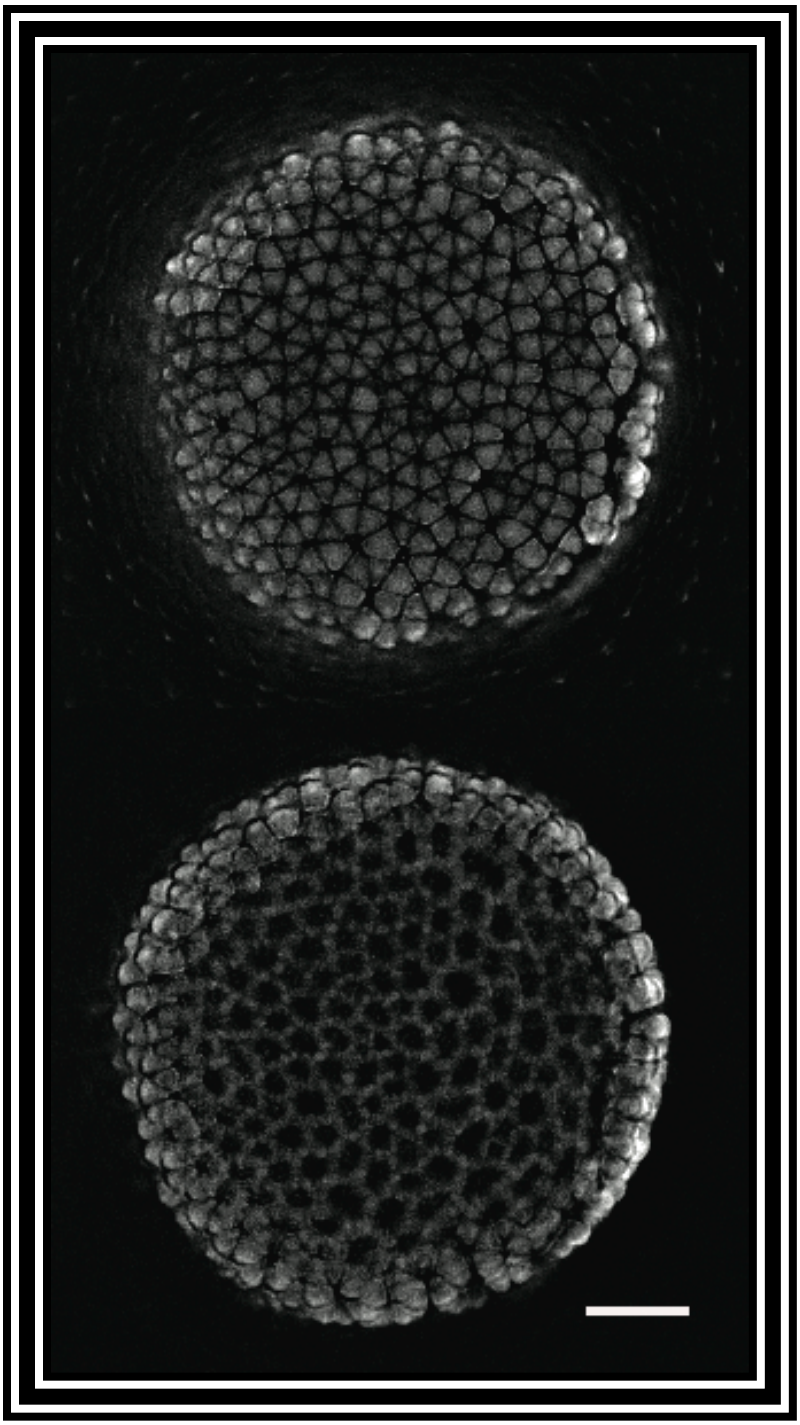

Figure 10. Superresolution Structured Illumination Microscopy (SR-SIM) images of the surface (top) and the basal cross-section of the clava (bottom) of a *Croton hirtellus* (Euphorbiaceae) pollen grain. The reticulate arrangement of the clava is evident thanks to the optical sectioning possible with SR-SIM. Scale bar represents 8 μm.

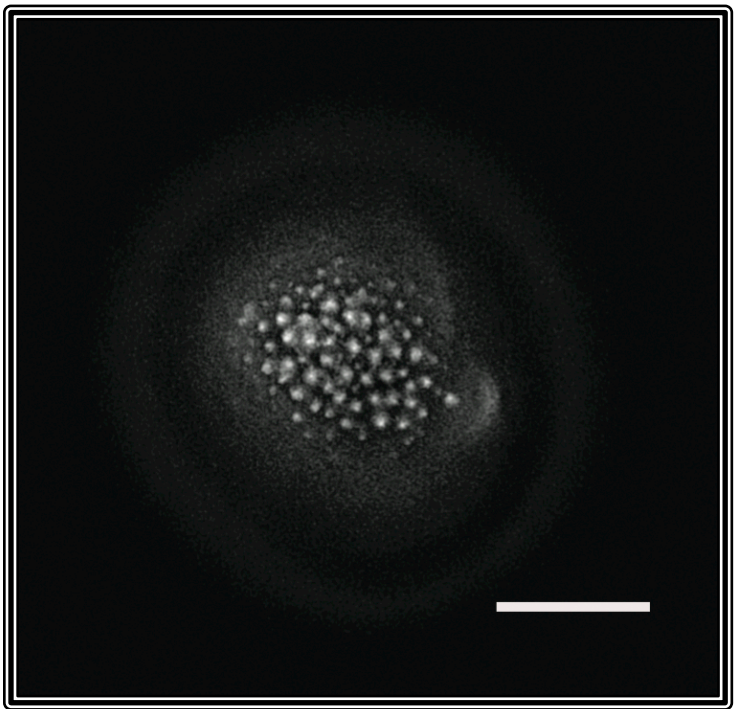

Figure 11. Superresolution Structured Illumination Microscopy (SR-SIM) image of the surface texture of an unknown species of grass pollen, demonstrating the contrast and resolution possible with modified sample preparation methods. This specimen was mounted on a slide in an aqueous-based mounting media instead of an oil-based mounting media and labeled with a fluorescent marker as opposed to not. Note the recovery of areolae and granulae at levels close to what the SEM can produce (Figure 2). Also note the morphology recovery differences between this image and the SR-SIM and LS-HR-DIC images taken of specimens prepared in the traditional oil-based, unlabeled method (Figure 8). Scale bar is 6.4 μm. Image courtesy of Mayandi Sivaguru.

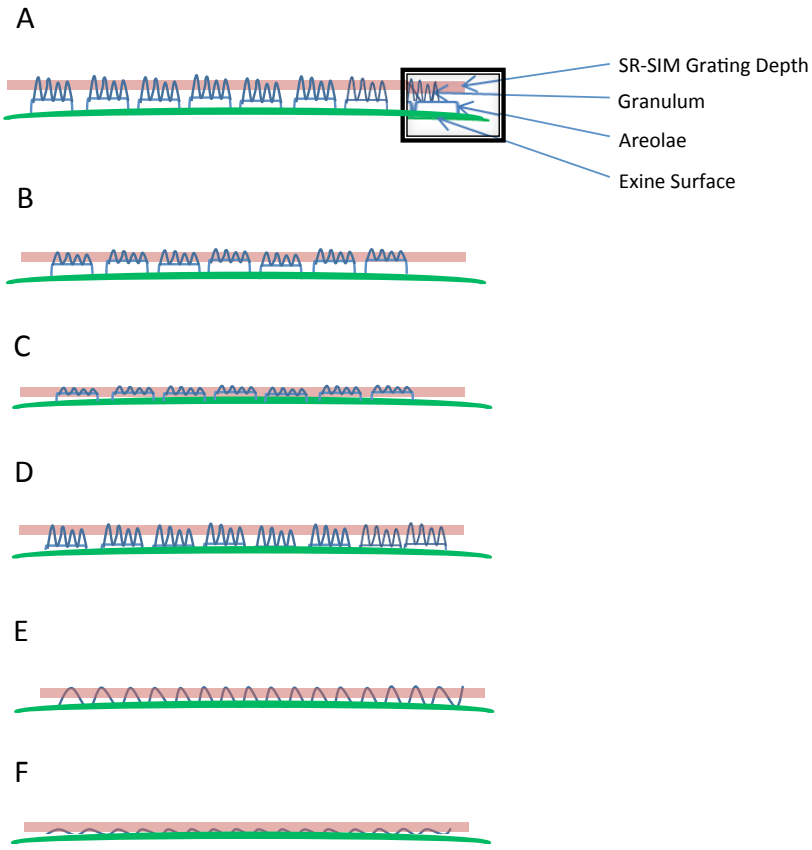

Figure 12. Inherent resolvability limitations of Superresolution Structured Illumination Microscopy (SR-SIM) due to the shallowness of pollen surface texture features and the depth of the SR-SIM grating (grid). A: innately high contrast between areolae and exine surface as well as between granulae and areolae generally indicates that granulae and areolae depth are greater than SR-SIM grating depth and therefore are resolvable. B: when pollen has innately high contrast between areolae and exine surface, but low contrast between granulae and areolae, then only the areolae are capable of being resolved. C: pollen with innately low contrast between areolae and exine surface as well as between granulae and areolae are not resolvable using SR-SIM due to these features being shallower than the SR-SIM grating. D: when pollen has innately high contrast between granulae and areolae, but low contrast between areolae and exine surface, then only the granulae are capable of being resolved. E: in the absence of areolae, but in the present of inherently high contrast between granulae and exine surface, then granulae will be resolved. F: in the absence of areolae, but in the present of inherently low contrast between granulae and exine surface, then granulae will not be resolved.

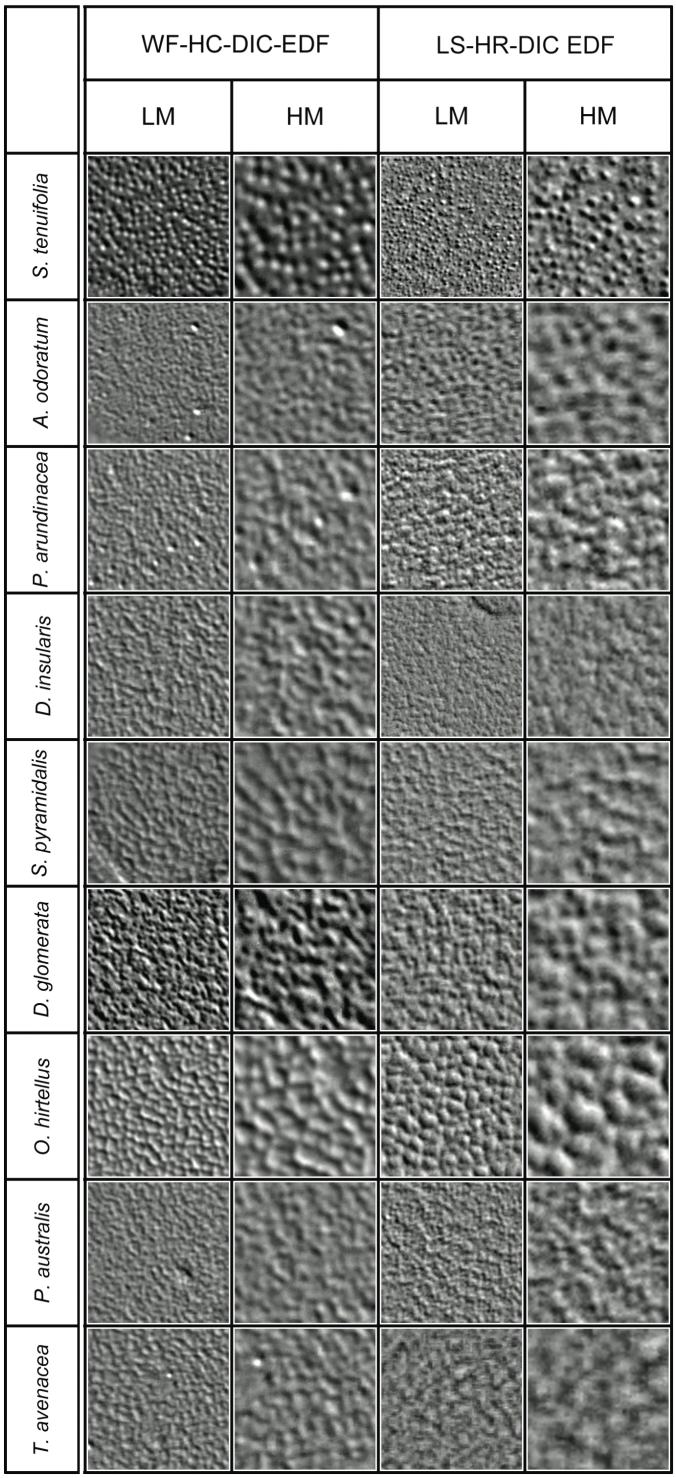

Figure 13. Extended Depth of Focus (EDF) images of Widefield High Contrast Differential Interference Contrast (DIC) and Laser-Scanning High-Resolution DIC Microscopy. These EDF images are compilations of all focal planes acquired in imaging pollen surface texture with DIC microscopy. LM and HM represent low magnification and high magnification, respectively. The Widefield High Contrast DIC LM images are 10 µm across and the HM images are 5 µm across. The Laser-Scanning High-Resolution DIC LM images are 6 µm across and the HM images are 3 µm across, except for *Anthoxanthum odoratum* and *Themeda avenacea*, which are 3 µm and 1.5 µm across for HM and LM, respectively.

Table 1

Grass species used in this study

Species	Poaceae Subfamily
Stipa tenuifolia	Pooideae
Anthoxanthum odoratum	Pooideae
Phalaris arundinacea	Pooideae
Digitaria insularis	Panicoideae
Sporobolus pyramidalis	Chloridoideae
Poa australis	Pooideae
Dactylis glomerata	Pooideae
Oplismenus hirtellus	Panicoideae
Themeda avenacea	Panicoideae

BIBLIOGRAPHY

Allen JR, ST Ross, MW Davidson 2014 Structured illumination microscopy for superresolution. ChemPhysChem Rev 15:566–76.

Andersen TS, F Bertelsen 1972 Scanning Electron Microscope Studies of Pollen of Cereals and other Grasses. Grana 12:79–86.

Atkin SL, S Barrier, Z Cui, PDI Fletcher, G Mackenzie, V Panel, V Sol, X Zhang 2011 UV and visible light screening by individual sporopollenin exines derived from Lycopodium clavatum (club moss) and Ambrosia trifida (giant ragweed). J Photochem Photobiol B Biol 102:209–217.

Beug H-J 2004 Leitfaden de Pollenbestimmung für Mitteleuropa und angrenzende Gebiete. München: Friedrich Pfeil.

Borel A, A Ollé, JM Vergès, R Sala 2014 Scanning Electron and Optical Light Microscopy: two complementary approaches for the understanding and interpretation of usewear and residues on stone tools. J Archaeol Sci 48:46–59.

Chaturvedi M, K Datta, PKK Nair 1998 Pollen morphology of Oryza (Poaceae). Grana 37:79–86.

Chen J, Y Xu, X Lv, X Lai, S Zeng 2013 Super-resolution differential interference contrast microscopy by structured illumination. Opt Express 21:112–121.

Dan D, B Yao, M Lei 2014 Structured Illumination Microscopy for Superresolution and Optical Sectioning. Chinese Sci Bull 59:1291–1307.

Dubertret B, P Skourides, DJ Norris, V Noireaux, AH Brivanlou, A Libchaber 2002 In vivo imaging of quantum dots encapsulated in phospholipid micelles. Science 298:1759–1762.

Fægri K, P Kaland, K Krzywinski, J Iversen 1989 Textbook of Pollen Analysis. 4th ed. New York: Wiley.

Fitzgibbon J, M Beck, J Zhou, C Faulkner, S Robatzek, K Oparka 2013 A developmental framework for complex plasmodesmata formation revealed by large-scale imaging of the Arabidopsis leaf epidermis. Plant Cell 25:57–70.

Fitzgibbon J, K Bell, E King, K Oparka 2010 Super-resolution imaging of plasmodesmata using three-dimensional structured illumination microscopy. Plant Physiol 153:1453–63.

Gustafsson MGL 2000 Surpassing the lateral resolution limit by a factor of two using structured illumination microscopy. J Microsc 198:82–7.

Gustafsson MGL, L Shao, PM Carlton, CJR Wang, IN Golubovskaya, WZ Cande, D a Agard, JW Sedat 2008 Three-dimensional resolution doubling in wide-field fluorescence microscopy by structured illumination. Biophys J 94:4957–70.

Habuchi S 2014 Super-Resolution Molecular and Functional Imaging of Nanoscale Architectures in Life and Materials Science. Front Bioeng Biotechnol 2:1–13.

Han R, Z Li, Y Fan, Y Jiang 2013 Recent advances in super-resolution fluorescence imaging and its applications in biology. J Genet Genomics 40:583–95.

Heintzmann R, G Ficz 2006 Breaking the resolution limit in light microscopy. Briefings Funct Genomics Proteomics 5:289–301.

Huang B, H Babcock, X Zhuang 2010 Breaking the diffraction barrier: super-resolution imaging of cells. Cell 143:1047–58.

Huang B, M Bates, X Zhuang 2009 Super-resolution fluorescence microscopy. Annu Rev Biochem 78:993–1016.

Inoué S, KR Spring 1997 Video Microscopy: The Fundamentals (The Language of Science). New York: Plenum Press.

Jost A, R Heintzmann 2013 Superresolution Multidimensional Imaging with Structured Illumination Microscopy. Annu Rev Mater Res 43:261–282.

Kasuboski JM, YJ Sigal, MS Joens, BF Lillemeier, JAJ Fitzpatrick 2012 Super-Resolution Microscopy: A Comparative Treatment. Curr Protoc Cytom 2:1–24.

Kirk S, J Skepper, A Donald 2009 Application of environmental scanning electron microscopy to determine biological surface structure. J Microsc 223:205–224.

Komis G, M Mistrik, O Samajová, A Doskočilová, M Ovečka, P Illés, J Bartek, J Samaj 2014 Dynamics and organization of cortical microtubules as revealed by superresolution structured illumination microscopy. Plant Physiol 165:129–48.

Kopek BG, G Shtengel, CS Xu, DA Clayton, HF Hess 2012 Correlative 3D superresolution fluorescence and electron microscopy reveal the relationship of mitochondrial nucleoids to membranes. Proc Natl Acad Sci U S A 109:6136–6141.

Leung BO, KC Chou 2011 Review of super-resolution fluorescence microscopy for biology. Appl Spectrosc 65:967–80.

Liesche J, I Ziomkiewicz, A Schulz 2013 Super-resolution imaging with Pontamine Fast Scarlet 4BS enables direct visualization of cellulose orientation and cell connection architecture in onion epidermis cells. BMC Plant Biol 13:226.

Linnik O, J Liesche, J Tilsner, KJ Oparka 2013 Unraveling the structure of viral replication complexes at super-resolution. Front Plant Sci 4:6.

Lomax BH, WT Fraser, MA Sephton, T V. Callaghan, S Self, M Harfoot, JA Pyle, CH Wellman, DJ Beerling 2008 Plant spore walls as a record of long-term changes in ultraviolet-B radiation. Nat Geosci 1:592–596.

Long BR, DC Robinson, H Zhong 2014 Subdiffractive microscopy: techniques, applications, and challenges. Wiley Interdiscip Rev Syst Biol Med 6:151–68.

Malkusch W, H Bauch, L Schäfer 2001 Digital light microscopy: Prerequisite for optimum contrast enhancement and increase of resolution. Exp Gerontol 36:1199–2117.

Mander L, M Li, W Mio, CC Fowlkes, SW Punyasena 2013 Classification of grass pollen through the quantitative analysis of surface ornamentation and texture. Proc R Soc B Biol Sci 280.

Mander L, S Punyasena 2014 On the Taxonomic Resolution of Pollen and Spore Records of Earth's Vegetation. Int J Plant Sci 175:931–945.

Muscariello L, F Rosso, G Marino, A Giordano, M Barbarisi, G Cafiero, A Barbarisi 2005 A Critical Overview of ESEM Applications in the Biological Field. J Cell Physiol 205:328–334.

Page J 1978 A scanning electron microscope survey of grass pollen. Kew Bull 32:313–319.

Peltre G, M-T Cerceau-Larrival, M Hideux, M Abadie, B David 1987 Scanning and transmission electron microscopy related to immunochemical analysis of grass pollen. Grana 26:158–170.

Punt W, P Hoen, S Blackmore, S Nilsson, A Le Thomas 2007 Glossary of pollen and spore terminology. Rev Palaeobot Palynol 143:1–81.

Rousseau D, Y Chéné, E Belin, G Semaan, G Trigui, K Boudehri, F Franconi, F Chapeau-Blondeau 2015 Multiscale imaging of plants: current approaches and challenges. Plant Methods 11:1–9.

Schermelleh L, R Heintzmann, H Leonhardt 2010 A guide to super-resolution fluorescence microscopy. J Cell Biol 190:165–75.

Schneider CA, WS Rasband, K. Eliceiri 2012 NIH Image to ImageJ: 25 years of image analysis. Nat Methods 9:671–675.

Sivaguru M, L Mander, G Fried, SW Punyasena 2012 Capturing the Surface Texture and Shape of Pollen: A Comparison of Microscopy Techniques. PLoS One 7:e39129.

Sozzani R, W Busch, EP Spalding, PN Benfey 2014 Advanced imaging techniques for the study of plant growth and development. Trends Plant Sci 19:304–10.

Strömberg CAE 2011 Evolution of Grasses and Grassland Ecosystems. Annu Rev Earth Planet Sci 39:517–544.

Traverse A 2007 Paleopalynology. 2nd ed. Springer Netherlands.

Weiss S 2000 Shattering the diffraction limit of light: A revolution in fluorescence microscopy? Proc Natl Acad Sci U S A 97:8747–8749.

Wodehouse RP 1935 Pollen grains. New York: McGraw Hill Book Company.